Proceedings World Geothermal Congress 2005
Antalya, Turkey, 24-29 April 2005

Magnetotelluric Survey in an Extremely Noisy Environment at the Pohang Low-Enthalpy Geothermal Area, Korea

Toshihiro Uchida[1], Yoonho Song[2], Tae Jong Lee[2], Yuji Mitsuhata[1], Seong-Keun Lim[2] and Seong Kon Lee[2]

[1]Institute for Geo-Resources and Environment, Geological Survey of Japan, AIST, Tsukuba 305-8567, Japan

[2]Korea Institute of Geoscience and Mineral Resources, 30 Gajeong-dong, Yuseong-gu, Daeeon 305-350, Korea

uchida-toshihiro@aist.go.jp

Keywords: magnetotelluric method, artificial noise, remote reference, 3D interpretation, Pohang, Korea, low-enthalpy geothermal resource

ABSTRACT

Korea is one of the most difficult countries in the world from the point of view of magnetotelluric (MT) data acquisition. This is because the natural MT signals are often completely contaminated by artificial electromagnetic noises from power lines and other various man-made sources. We conducted MT measurements in the Pohang area, southeastern Korea, in 2002 and 2003, as one of the initial surveys for the development of low-enthalpy geothermal resources in the area. We applied a very far remote reference by setting a remote site in southwestern Japan, which is approximately 500 km away from the Pohang area. Very strong artificial noise was observed at a frequency band from 0.1 Hz to 100 Hz. The remote reference processing successfully removed most of these noises. Although the resultant MT impedance was not of very high quality at most sites as compared with the clean data obtained in calm areas in other countries, these data are of sufficient quality for further interpretation. We carried out 3D inversion of the MT data and compared with geological and drilling data in the area. In this paper, we present the remote referenced results and the 3D resistivity models of the Pohang geothermal area.

1. INTRODUCTION

Korea is one of the most difficult countries for magnetotelluric (MT) measurement because artificial electromagnetic (EM) noises are extremely strong over almost the whole country. Two possible reasons are as follows: 1) the power line systems, which seem to be the major noise sources, cover almost the entire country, even in country-side farming areas, and 2) the country is mostly underlain by relatively old sedimentary formations and granitic rocks that generally have high resistivity, through which the EM noises can propagate to great distances. These conditions have prevented EM researchers in Korea from obtaining good-quality MT data for years.

The remote-reference analysis has been a standard technique for the MT data processing to remove local EM noises that exist only in the vicinity of the survey area (Gamble et al., 1979). However, when there is a DC noise source, such as a DC train system or a DC high-voltage power transmission line, we often observe step-like noises that have a wide frequency spectrum. Such noises can propagate to a great distance, hence we have to separate the remote station to be far away, say more than 100 km from the survey area, to remove the noises with the remote-reference process. There have been several successful case studies reported on this problem in Japan, Italy, etc. (e.g., Takasugi and Muramatsu, 1991; Takakura et al., 1994; Fiordelisi et al., 1995).

In this work, we have conducted an MT survey in the Pohang low-enthalpy geothermal area, southeastern Korea. The field work was carried out in 2002 and 2003 under a joint research project between the Korea Institute of Geoscience and Mineral Resources (KIGAM) and the Institute for Geo-Resources and Environment (GREEN), Geological Survey of Japan (GSJ), AIST. As the first trial of the remote-reference MT survey in Korea, we deployed a remote station in Korea. In addition, we utilized other remote-reference data that were obtained in Kyushu, Japan, at the same time. By using these reference data, the quality of the MT data was improved dramatically. We then conducted three-dimensional (3D) inversions and carried out some interpretation for low-enthalpy geothermal resources in the Pohang area.

2. MT SURVEY IN POHANG

2.1 Pohang Area

The survey area is located in the north of Pohang City, southeastern Korea (Figure 1). The main lineament structure in this area is the NNE-SSW trending Yangsan Fault, which runs west of the survey area (Figure 2; Song et al., 2003). Many other small lineaments that are parallel with or in the conjugate directions to the Yangsan Fault can be recognized from a satellite image. The major formations to the west of the Yangsan Fault are sedimentary and granitic rocks from Cretaceous time, while the area to the east of the Yangsan Fault is mostly underlain by Tertiary sedimentary formations that are expected to be underlain by the Cretaceous granitic formations. There is a small basin structure around Heung-Hae Town, which is covered by Quaternary alluvium. The main target of the geothermal exploration and the MT survey was set in the southern side of the basin, where two minor lineaments in NNE-SSW and WNW-ESE directions intersect.

2.2 MT survey

MT stations were deployed around the Heung-Hae basin, mostly concentrated in the southern side of the basin (Figure 3). The number of MT sites was 70, 33 of which were measured in 2002 and 37 in 2003. For the remote reference sites in Korea, we set one in a mountainous area in the Andong Province in 2002 (K-1 in Figure 1) and another at a place near Daejeon City in 2003 (K-2 in Figure 1). The straight distance from the survey area was approximately 60 km to K-1 and 170 km to K-2. The remote reference site in Japan was located near the Ogiri geothermal field in southern Kyushu Island, southwestern Japan (J-1 in Figure 1). The distance between the site J-1 and the survey area was approximately 500 km.

For the MT measurement, both magnetic sensor *Hx* and electric dipole *Ex* were oriented to magnetic north (-7 degrees) at all sites in Korea, while the magnetic sensor *Hx* was oriented to a direction of –27 degrees at J-1 in Japan. The power line frequency is 60 Hz both in Korea and western Japan. The recording time for the low frequency band was 15 hours, from evening to the next morning. The synchronization among all the instruments was maintained by using GPS clock signals. We carried out the measurement for two nights at each station in the survey area.

3. REMOTE REFERENCE ANALYSIS

3.1 Time Series Data

Figure 4 shows examples of time series segments of two electric fields, *Ex* and *Ey*, and three magnetic fields, *Hx*, *Hy* and *Hz*, at Station 111, K-1 and J-1 on November 2, 2002. In the middle-frequency band (Figure 4a), we can recognize two kinds of noise in all five components at Station 111, which is located at the middle of the survey area (Figure 3). The first one is a high-frequency, continuous, pulse-like noise of smaller amplitude at about 20 Hz. The other is also a pulse-like noise of larger amplitude at about every 0.5 s, whose interval is irregular. These noises seem to be observed throughout the recording time from the evening to the next morning. We interpret that they are caused by some artificial noise sources such as leakage currents from power line systems.

At the remote station K-1, such noises were not recorded. The amplitude of the electric fields is very large because the subsurface is more resistive at this remote station than in the survey area. The time series data at the remote station J-1 in Japan have smaller amplitudes for both electric and magnetic fields than those at Station 111. Nevertheless, we can trace similar events in the magnetic fields between K-1 and J-1, particularly in *Hx*. These magnetic data seem to contain signals at 8 Hz, which is one of the Schumann resonance frequencies. We must notice that the *x* and *y* directions, respectively, are 20 degrees different between the Korean stations and J-1.

In the low-frequency band (Figure 4b), we can recognize very good correlation in magnetic field data among the three stations 111, K-1 and J-1, except the noisy *Hz* data at Station 111. The dominant period of these signals is some tens of seconds, which is typical of the ultra-low-frequency (ULF) pulsation signals. The electric fields, however, are different among the stations, depending on the underground resistivity and noise. The amplitude of *Ey* data at the station K-1 is greater than *Ex*, which is due to the sea effect from the Sea of Japan (East Sea).

3.2 MT Impedances

Figure 5 compares MT impedances (apparent resistivities and phases) at Station 111 among single-site process, remote-reference process with Station K-1, remote-reference process with Station J-1, and edited data after the process with J-1. In the single-site impedance curves, we can recognize near-field noises at frequencies from 0.1 Hz to 10 Hz, where the phases are almost zero (or -180 degrees) in both components of *xy* and *yx* and the apparent resistivity curve of the *xy* component has a steep gradient of about 45 degrees. Most of these noises were removed by the remote-reference analysis with K-1, except that ambiguous noises remain between 0.1 Hz and 1 Hz. However, this portion was improved by the reference analysis with J-1.

Figure 6 compares MT impedances at Station 209. This is one of the worst quality sites in the survey area. We can recognize severe near-field noises from low frequency (approximately 0.1 Hz) to high frequency (approximately 100 Hz), where phase values are close to zero. Even after the remote reference analysis with K-1 or J-1, the resultant impedances at these frequencies are of bad quality.

Figures 5d and 6d shows edited MT impedances (referenced with J-1), in which outlier segments or large-variance segments were removed manually. If strong noises exist only within specific time segments in the 15 hours of recording, we can improve the final data quality by eliminating those bad segments. For example, data quality from 1 Hz o 10 Hz at Station 209 was improved very much (Figures 6d). On the other hand, the improvement for Station 111 was not as significant (Figures 5d).

In fact, average data quality was better in the 2002 data than in 2003. This was because the signal strength in the ULF band was generally low during the 2003 survey. The overall data quality seems to be sufficient for further interpretation, although these data are not very good even after the reference analysis with J-1 if we compare them with high-quality data obtained in calm geothermal fields in Japan and other countries. We used the edited version of the data at all stations for further interpretation.

3.3 Induction Vectors

Figure 7 shows induction vectors at three frequencies: 8 Hz, 0.3 Hz and 0.01 Hz. They are drawn with a convention that they point toward a low-resistivity zone. At 8 Hz, lengths of the vectors are small and the directions are not systematic among stations. This means that the shallow portion has weak resistivity change in a horizontal direction and is nearly one-dimensional. A rough average of apparent resistivities at 8 Hz is 10 ohm-m. That corresponds to a skin depth of approximately 500 m.

The induction vectors at 0.3 Hz have an amplitude of 0.3 - 0.5 and point toward the south. The skin depth of this frequency is approximately 3 - 4 km. This means that a large low-resistivity body exists to the south of the survey area at a distance and/or a depth of 3 - 4 km. This may cause a problem when we conduct 2D interpretation along east-west survey lines because the strike direction is parallel to the survey line at this frequency.

When the frequency is much lower, the induction vectors point toward the east, where the Sea of Japan (East Sea) is located. The amplitude at 0.01 Hz is 0.5 or greater. To interpret the data at 0.01 Hz and below, we must include the sea in the 2D or 3D models.

4. 3D INTERPRETATION

4.1 3D Inversion

Based on the existing survey data including the MT data in 2002, KIGAM chose a site for pilot drillings in the southern part of the survey area in early 2003. In fact, the MT sites in the 2003 survey were densely arranged around the drilling site (Figure 3).

We set a zone for 3D interpretation surrounding the drilling site (Figure 3). The number of MT sites used for the 3D inversion was 44. The number of frequencies used was 11; from 0.063 Hz to 66 Hz. The impedances were rotated to a direction of 0 degree, and the off-diagonal components of the MT impedance were utilized in the inversion. The finite-difference method was used for the 3D forward

computation and the linearized least-squares inversion with optimum smoothness regularization was used for the inversion (Sasaki, 1999; Uchida and Sasaki, 2003; Sasaki, 2004). The cell sizes in the horizontal and vertical directions were 150 m and 50 m, respectively, at the surface in the interpreted area. To compensate for the sea effect on the MT impedance, a shallow low-resistivity layer of 0.3 ohm-m and a thickness of 100 m was inserted in the eastern side of the mesh to represent the sea water. The size of the blocks for the inversion was 300 m horizontally at the surface. A noise floor of 1% was assumed. Since the static shifts were not significant for these sites, they were not considered in the 3D inversion.

Figure 8 shows depth-slice sections of the final 3D model. The survey area is underlain by a low-resistivity layer, whose resistivity is 10 ohm-m or less. The thickness of this layer is small (200 - 300 m) in the north of the survey area and it becomes thicker to the south. The thickest zone (approximately 1000 m) is located in the south-center portion of the area. Below is a high-resistivity layer of approximately 100 ohm-m, which is distributed over the whole survey area. At depths greater than 3 km, a deep low-resistivity anomaly is obtained in the southern part of the survey area. Figure 9 shows two 3D volume models, in which the 3D volume is cut at planes of x = 2.25 km and y = 1.65 km, which approximately pass the location of the two boreholes. These boreholes reached the high-resistivity second layer.

4.2 Comparison with Geology and Logging Data

Figure 10 shows the geologic structure estimated from the drilling results of BH-1 and BH-2. The geologic column in BH-2 from the surface is semi-consolidated mudstone (0 - 352 m), mixed zone of basalt, tuff and mudstone (352 - 525 m), intruded rhyolite (525 - 900 m), and sandstone and mudstone in Cretaceous time (900 - bottom). Geology in BH-1 is similar to that in BH-2.

Figure 11 compares the 3D resistivity model with electrical logging data in BH-2. The surface semi-consolidated mudstone has low-resistivity (10 ohm-m or less) from the logging data, which corresponds to the surface low-resistivity layer in the 3D resistivity model. The rhyolite layer shows high-resistivity (several hundreds ohm-m) from the logging. However, the 3D model can not properly indicate it, only showing 30 - 60 ohm-m at depths from 500 m to 900 m. The deep sandstone/mudstone layer has several tens of ohm-m from the logging, with which the 3D model is consistent.

The 3D model in Figure 9 clearly shows the lower boundary of the semi-consolidated mudstone (surface low-resistivity layer). Two boreholes were drilled on a north-south slope of this boundary (left panel, Figure 9). High-resistivity layers of rhyolite and deep sandstone/mudstone are interpreted as a single high-resistivity zone from several tens ohm-m to 100 ohm-m. The 3D model does not have sufficient resolution to distinguish these resistive layers.

A deep low-resistivity zone is obtained in the south of the survey area. However its existence is still uncertain because of the small sensitivity of the data with regard to those deep blocks. Although the sea water is included in the model on the eastern side of the finite difference mesh, accurate modeling of the bathymetry has not yet been conducted. Therefore, the model has an ambiguity for the deeper portion. Nevertheless, the low-resistivity zone seems to support the trend of induction vectors at 0.3 Hz, which generally point southward.

We have also conducted 2D interpretation for five east-west lines and two NNE-SSW lines, by connecting neighboring stations along those directions (not shown in this paper). So-called TM-mode data were used. Although the final data misfits from the 2D and 3D inversions are at a similar level, 2D models of the east-west lines show much smaller resistivity values than the logging data for the blocks that correspond to the deep high-resistivity zone of BH-2. 2D models of the NNE-SSW lines created an ambiguous resistive anomaly in a deeper portion in the south. From these observations, the 3D models seem to be more reliable.

According to temperature logging in BH-2, the highest temperature obtained was approximately 65 degrees at the well bottom. Resistivity structure in a high-enthalpy geothermal field usually depends on clay minerals and temperature as well as formation lithology (e.g., Uchida and Sasaki, 2003). In this survey area, however, temperature is not very high and hydrothermal clay minerals are not significant in the drilling data. Therefore, the main role of the 3D resistivity model is to provide the shapes of formation boundaries and major resistivity anomalies, from which we can estimate typical geological features such as faults and lineaments. From that point of view, we can interpret that the two boreholes are close to a west-east trending resistivity boundary at depths from 1 to 2 km (left panel, Figure 9). Also, the boreholes are located in a small north-south trending valley beneath the low-resistivity semi-consolidated mudstone (right panel, Figure 9). There are a few major fracture zones found in the Cretaceous sedimentary layers in BH-2. A long-term production experiment is planned in 2004.

5. CONCLUSIONS

We conducted a far remote-reference MT measurement in the Pohang geothermal area, southeastern Korea. Strong artificial EM noises were observed in time series data at all stations. By a remote-reference analysis with a remote station either in Korea or Japan, most of those noises could be removed properly. The resultant MT impedance data have a sufficient quality for further interpretation. Our experiment has revealed a good possibility of utilizing the MT method in Korea.

Preliminary resistivity structures were obtained by 3D inversions of the MT data. To deal with the sea effect, a sea water zone was included in the finite difference mesh. The final 3D model indicated a shallow low-resistivity layer of less than 10 ohm-m whose depth varies from 200 m in the north to 1000 m in the south. This layer corresponds to a semi-consolidated mudstone in Tertiary time. Below that is a high-resistivity layer of approximately 100 ohm-m. This corresponds to Cretaceous sandstone/mudstone and Tertiary rhyolite intrusion. Although the rhyolite layer has high resistivity (several hundreds of ohm-m by electrical logging), the MT model could not resolve such a high-resistivity value because of the existence of the low-resistivity surface layer above.

ACKNOWLEDGMENTS

This work was conducted under a joint research project between KIGAM and GREEN-GSJ-AIST. The reference data in Japan in 2002 were obtained under a project of Tottori Prefectural Government for earthquake studies. The authors thank all the participants of the MT field work: Toru Mogi, In Hwa Park, Seong Jun Cho, Jeong Sul Son, Heuisoon Lee, Hoon Gil Kim, and students at Seoul National University and Chonbuk National University.

REFERENCES

Fiordelisi, A., Mackie, R., Madden, T., Manzella, A., and Rieven, S.: Application of magnetotelluric method using a remote-remote-reference system for characterising deep geothermal system, *Proc. of World Geothermal Congress 1995*, (1995), Vol. 2, 893-898.

Gamble, T. D., Goubau, W. M., and Clarke, J.: Magnetotellurics with a remote reference, *Geophysics*, **44**, (1979), 53-68.

Sasaki, Y.: 3-D inversion of electrical and electromagnetic data on PC, *Proc. of 2nd International Symposium on Three-Dimensional Electromagnetics*, (1999), 128-131.

Sasaki, Y.: Three-dimensional inversion of static-shifted magnetotelluric data, *Earth, Planets and Space*, **56**, (2004), 239-248.

Song, Y., Lee, S. K., Kim, H. C., Kee, W.-S., Park, Y.-S., Lim, M.-T., Son, J.-S., Cho, S.-J., Lim, S.-K., Uchida, T., Mitsuhata, Y., Lee, T. J., Lee, H., Rim H.-R., Hwang, S., and Park, I.-H.: Low-enthalpy geothermal exploration in Pohang area, Korea, *Proceedings of the International Symposium on the Fusion Technology of Geosystem Engineering, Rock Engineering and Geophysical Exploration*, (2003), 470-475.

Takakura S., Takeda, M., and Matsuo, K.: Effects of regional noise on magnetotellurics and their removal by far remote reference method, *Geophys. Explorer. (Butsuri Tansa)*, **47**, (1994), 24-35 (in Japanese with English abstract).

Takasugi S., and and Muramatsu, S.: Data processing techniques designed to improve MT data quality, *Geophys. Explorer. (Butsuri Tansa)*, **44**, (1991), 126-137.

Uchida, T., and Sasaki, Y.: Stable 3-D inversion of MT data and its application to geothermal exploration: *in* Macnae, J. and Liu, G. (eds.), *Three-Dimensional Electromagnetics III*, ASEG, (2003), 12.1-12.10.

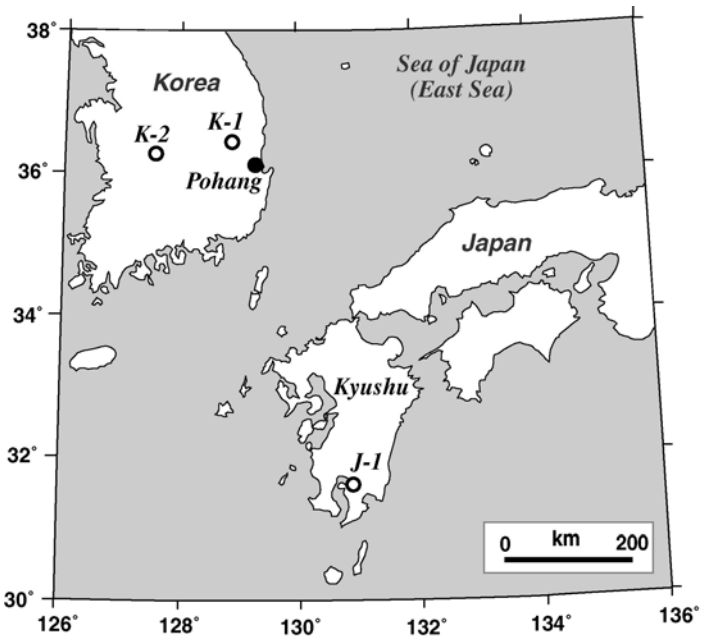

Figure 1: Location of the Pohang low-enthalpy geothermal area (solid circle), southeastern Korea. Open circles are remote-reference stations in Korea (K-1 and K-2) and Japan (J-1).

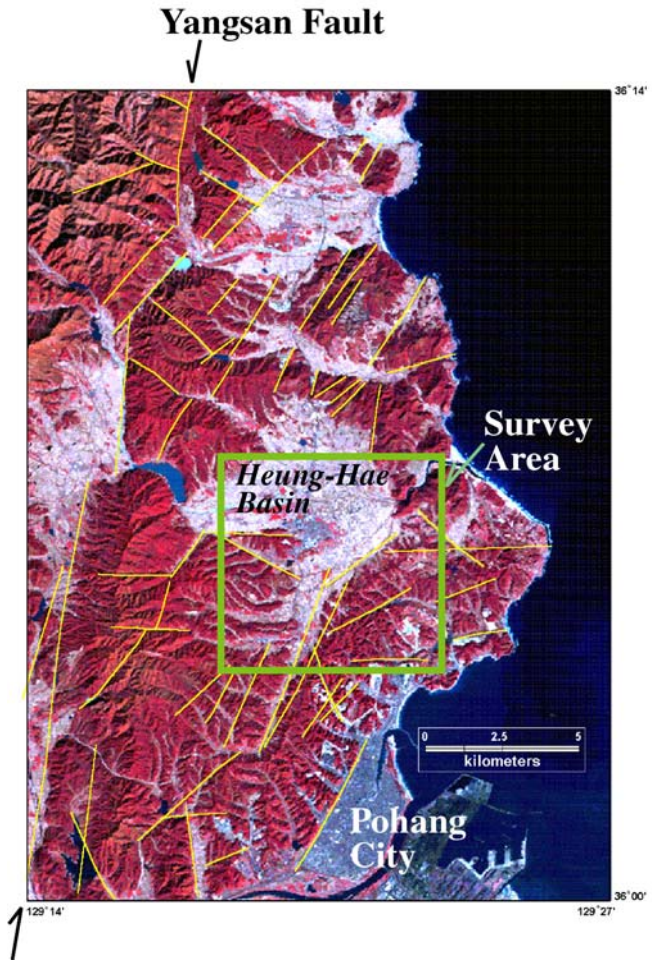

Figure 2. Location of the survey area (the green rectangle) on a satellite image (Song et al., 2003). Thin yellow lines are estimated lineaments from the image.

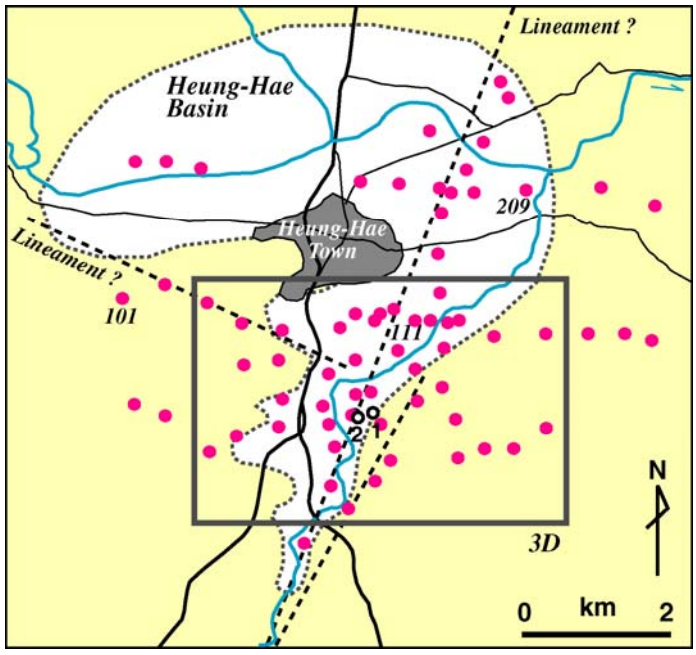

Figure 3. Location of MT stations in the Pohang area. Red dots are MT stations, the gray shaded area is Heung-Hae Town, black solid lines are roads, blue solid lines are rivers, thick dashed lines are estimated lineaments, and the thin dotted line is the boundary of the basin structure. A large rectangle indicates the zone for 3D interpretation.

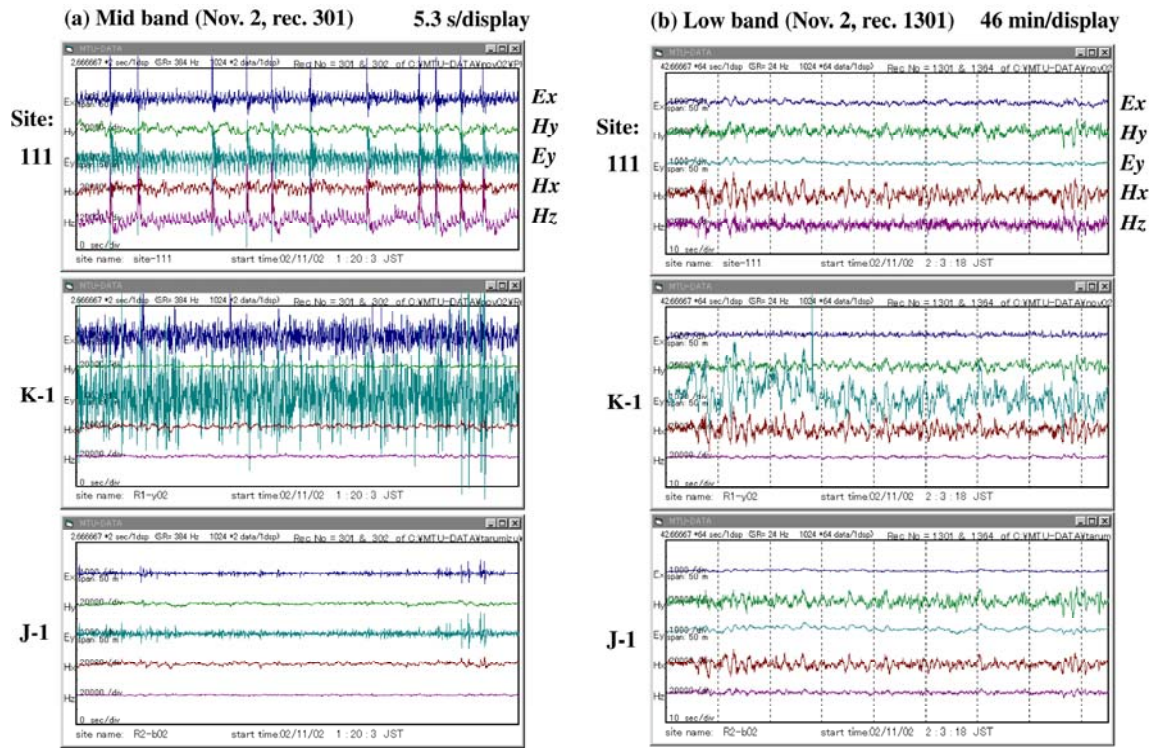

Figure 4. Examples of raw time-series data of two electric fields and three magnetic fields at Stations 111, K-1 and J-1 on November 2, 2002: (a) middle-frequency band, and (b) low-frequency band. Window length is 5.3 seconds for the middle band and 46 minutes for the low band. Sampling rate is 384 Hz for the middle band and 24 Hz for the low band. Vertical scale is 1000 points/div for electric fields and 20000 points/div for magnetic fields.

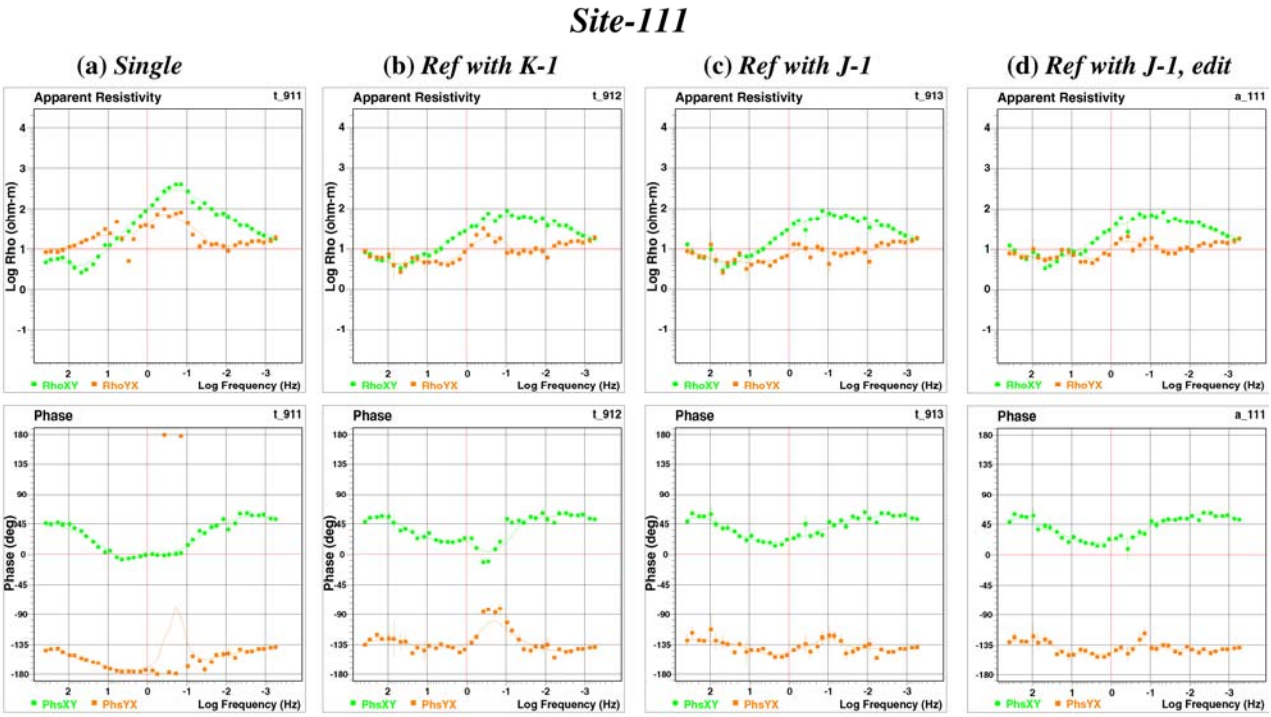

Figure 5. Apparent resistivity and phase curves at Station 111 with (a) single-site process, (b) remote reference with K-1 in Korea, (c) remote reference with J-1 in Japan, and (d) edited data after reference with J-1. Circles (green) are the *xy*-component, and squares (orange) are *yx*-component. *x*-direction is true north.

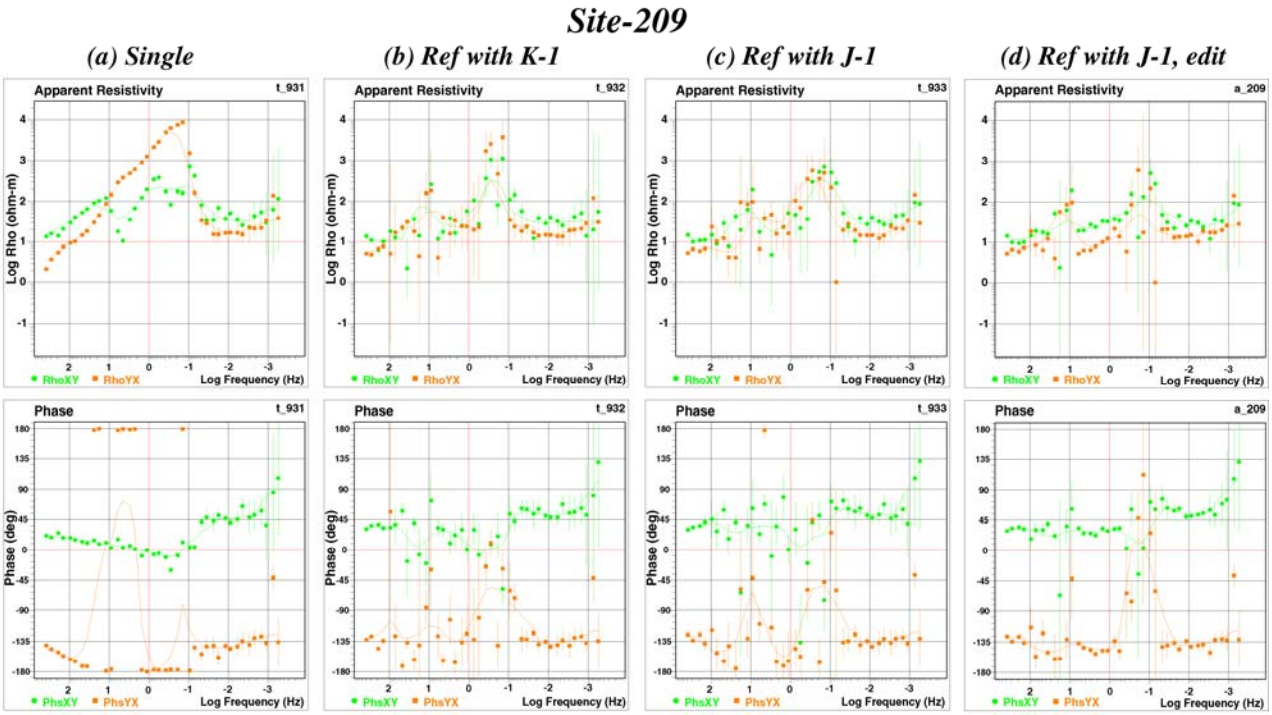

Figure 6. Apparent resistivity and phase curves at Station 209 with (a) single-site process, (b) remote reference with K-1 in Korea, (c) remote reference with J-1 in Japan, and (d) edited data after reference with J-1. Circles (green) are the *xy*-component, and squares (orange) are *yx*-component.

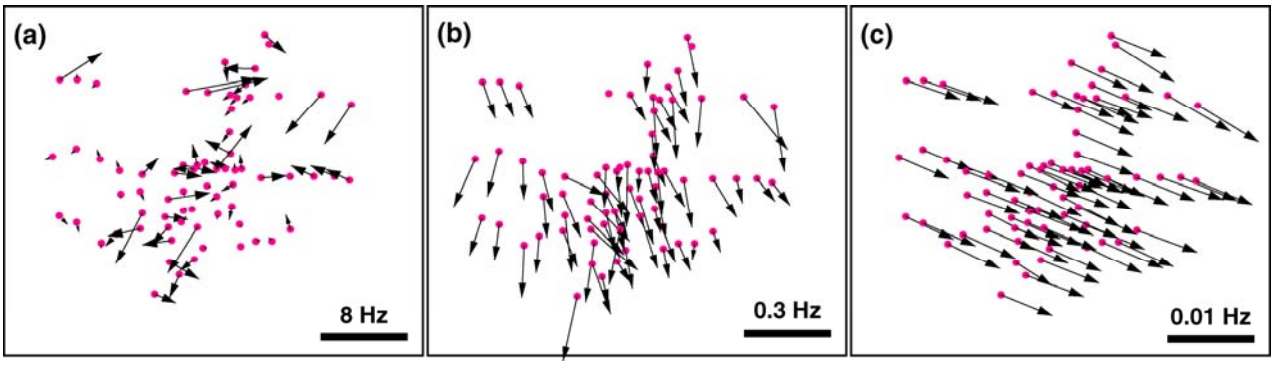

Figure 7. Induction vectors at (a) 8 Hz, (b) 0.3 Hz, and (c) 0.01 Hz. Length of a thick black bar indicates a unit amplitude of a vector. Arrows point towards a low-resistivity zone. Extremely noisy data were omitted. North is upward.

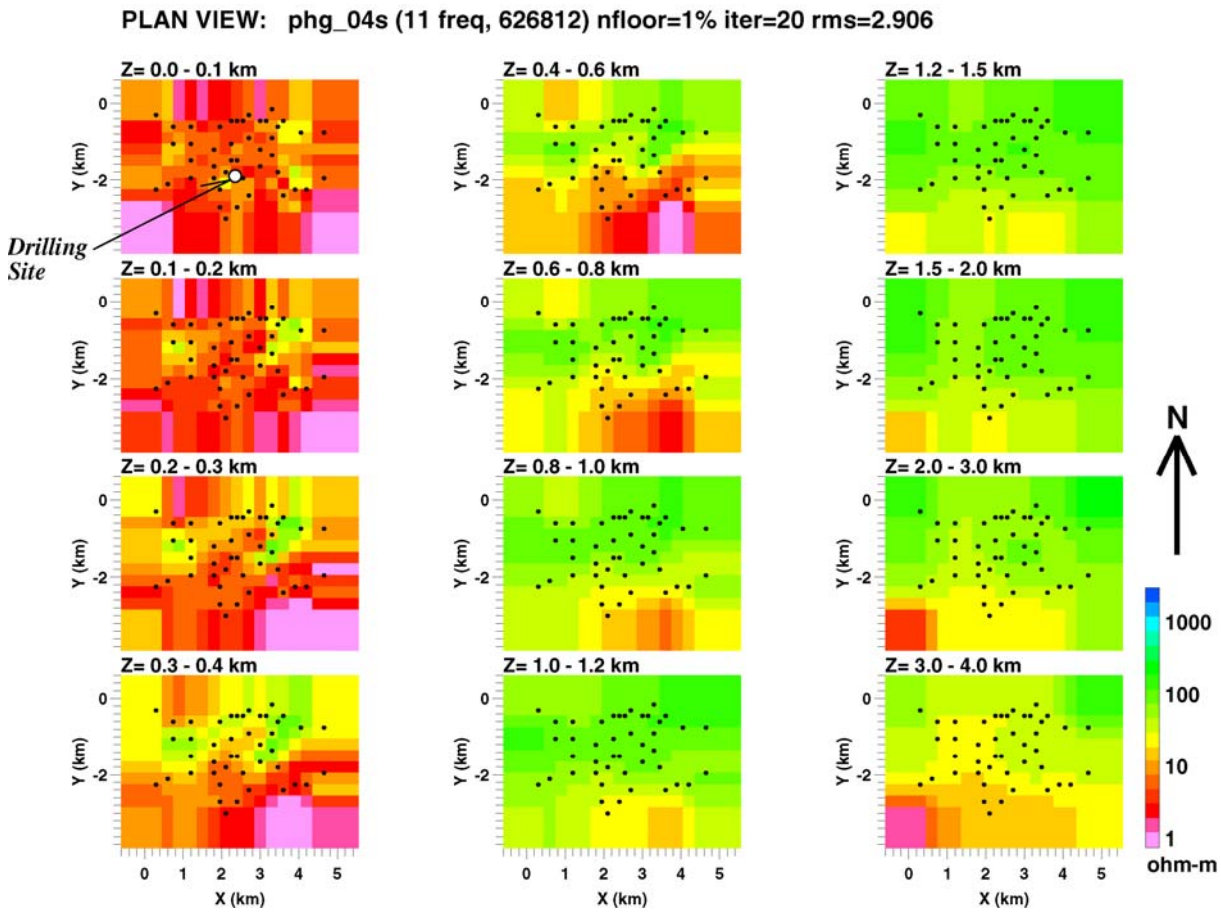

Figure 8. Depth-slice resistivity sections of a 3D inverted model. The area for the 3D interpretation is shown in Figure 3. Black dots are MT stations. The open circle indicates the drilling site.

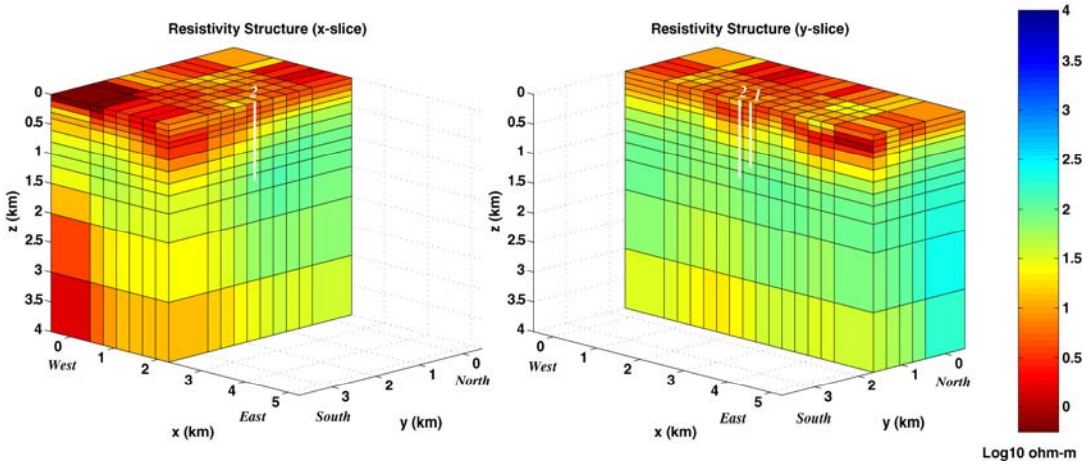

Figure 9. 3D view of the resistivity model. The volume is cut at an x-plane (x = 2.25 km) (left panel) and a y-plane (y = 1.65 km) (right panel). White bars indicate pilot drillings.

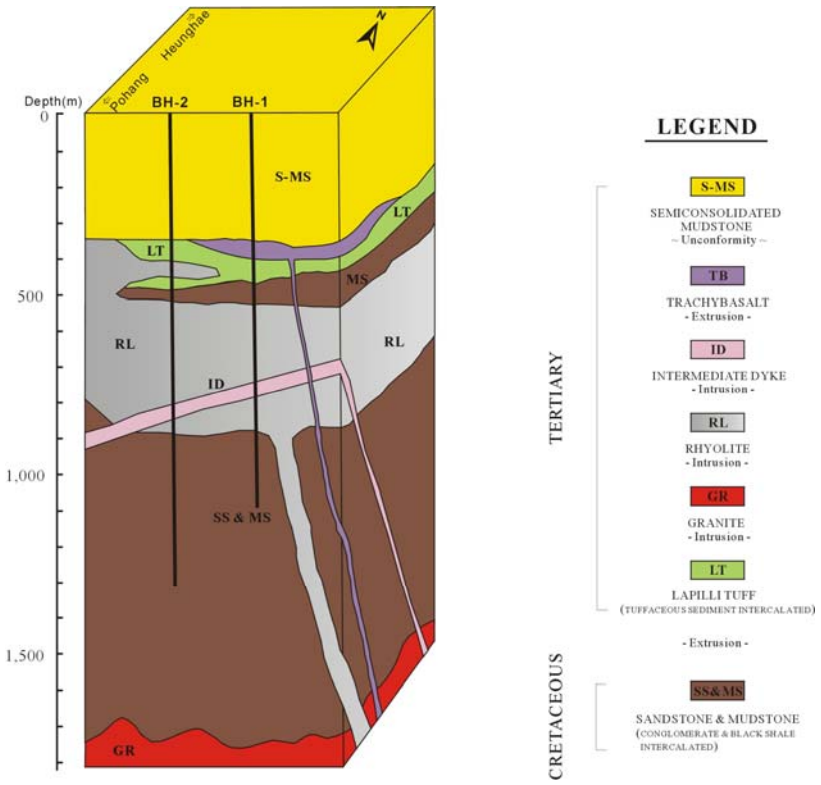

Figure 10. Geology model obtained from the drilling data of BH-1 and BH-2.

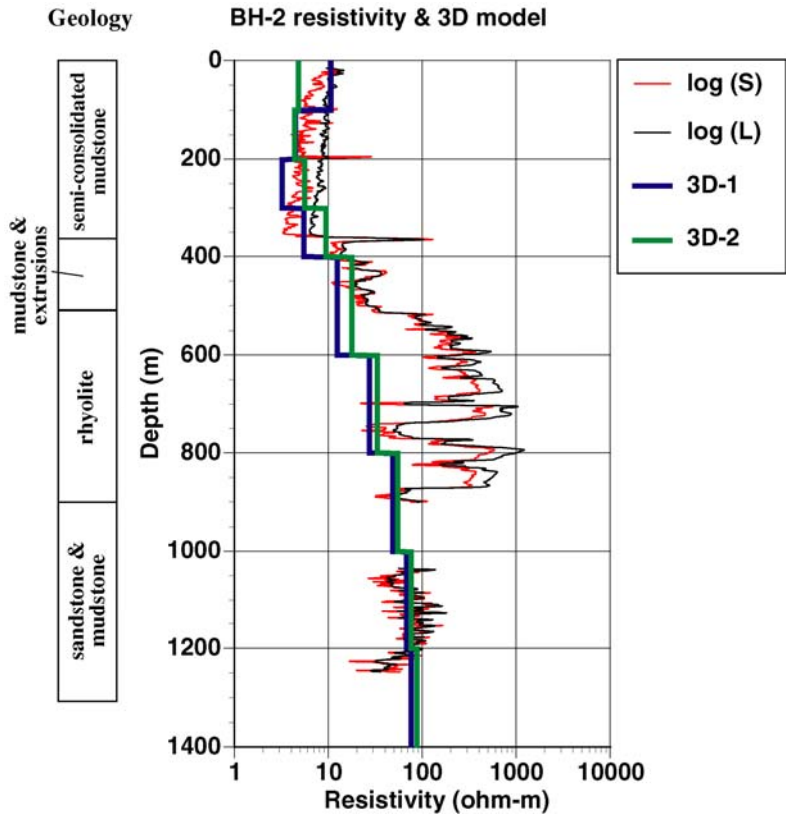

Figure 11. Comparison of 3D resistivity model of the MT data with the resistivity logging data in BH-2. Red line is short normal, black line is long normal, thick blue and green lines are from the blocks near the borehole in the 3D model. Simplified geologic column in BH-2 is also shown.